Effects of Temperature on Chaotropic Anion-Induced Shape Transitions of Star Molecular Bottlebrushes with Heterografted Poly(ethylene oxide) and Poly(*N*,*N*-dialkylaminoethyl methacrylate) Side Chains in Acidic Water

*Evan M. Lewoczko, Michael T. Kelly, Ethan W. Kent, and Bin Zhao**

Department of Chemistry, University of Tennessee, Knoxville, Tennessee 37996, United States

* Corresponding author. Email: bzhao@utk.edu

Abstract. This article reports a study of the effects of temperature on chaotropic anion (CA)-induced star-globule shape transitions in acidic water of three-arm star bottlebrushes composed of heterografted poly(ethylene oxide) (PEO) and either poly(2-(*N*,*N*-dimethylamino)ethyl methacrylate) (PDMAEMA) or poly(2-(*N*,*N*-diethylamino)ethyl methacrylate) (PDEAEMA) (the brushes denoted as SMB-11 and -22, respectively). The brush polymers were synthesized by grafting alkyne-end-functionalized PEO and PDMAEMA or PDEAEMA onto an azide-bearing three-arm star backbone polymer using the copper(I)-catalyzed alkyne-azide cycloaddition reaction. Six anions were studied for their effects on the conformations of SMB-11 and -22 in acidic water: super CAs $[Fe(CN)_6]^{3-}$ and $[Fe(CN)_6]^{4-}$, moderate CAs PF_6^- and ClO_4^-, weak CA I^-, and for comparison, kosmotropic anion SO_4^{2-}. At 25 °C, the addition of super and moderate CAs induced shape transitions of SMB-11 and -22 in pH 4.50 water from a starlike to a collapsed globular state stabilized by PEO side chains, which was driven by the ion pairing of protonated tertiary amine groups with CAs and the chaotropic effect. The shape changes occurred at much lower salt concentrations for super CAs than moderate CAs. Upon heating from near room

temperature to 70 °C, the super CA-collapsed brushes remained in the globular state, whereas the moderate CA-collapsed brushes underwent reversible globule-to-star shape transitions. The transition temperature increased with increasing salt concentration and was found to be higher for SMB-22 at the same salt concentration, presumably caused by the chaotropic effect. In contrast, I^- and SO_4^{2-} had small effects on the conformations of SMB-11 and -22 at 25 °C in the studied salt concentration range, and only small and gradual size variations were observed upon heating to 70 °C. The results reported here may have potential uses in the design of stimuli-responsive systems for substance encapsulation and release.

Introduction

Molecular bottlebrushes (MBBs), also called brush polymers, are composed of one or more types of relatively short polymeric side chains covalently grafted on a backbone polymer with a sufficiently high grafting density.[1-7] These architecturally complex polymers have received tremendous interest in recent years owing to their unique structural characteristics, intriguing behavior, and potential applications in a wide variety of areas including drug delivery,[8] aqueous lubrication,[9] and fabrication of photonic crystals and supersoft elastomers.[7,10] The unique characteristics and behavior of MBBs, such as high density of functional groups, large and tunable persistence length,[2,3] lack of main chain entanglement,[7] and unusual crystal habit,[11] originate mainly from the high grafting density of macromolecular side chains on the backbone. At a sufficiently high aspect ratio, linear MBBs take on an extended wormlike morphology in good solvents due to excluded volume interactions,[1-5] which can be visualized by atomic force microscopy (AFM) and transmission electron microscopy. When the environmental conditions change, MBBs can exhibit marked shape transitions,[2,3,5] e.g., from wormlike or starlike to globular.

Although intriguing worm-globule shape transitions of MBBs have been shown at air-water interfaces by lateral compression and on solid substrates by exposure to different solvent vapors, [12-14] stimuli-responsive shape-changing MBBs in solution are more relevant to potential applications such as encapsulation and release of substances.[3,5,15] These brush polymers are commonly synthesized with the use of stimuli-responsive polymers that exhibit a large and abrupt conformational transition, often accompanied with a solubility change in solution, in response to external stimuli, such as a change in pH, temperature or solvent, addition of a specific ion, and light.[15-28] Schmidt et al. synthesized the first thermoresponsive linear MBBs using a "grafting from" method via atom transfer radical polymerization (ATRP) to grow poly(*N*-isopropylacrylamide)

(PNIPAm) side chains from a long macroinitiator with pendant initiating moieties.[15] The PNIPAm brush polymer was observed by AFM to exhibit a pronounced worm-to-globule shape transition in water upon heating. However, above the lower critical solution temperature (LCST), the collapsed globular brushes were unstable and underwent aggregation and precipitation in the solution. Polyelectrolyte MBBs can undergo large conformational transitions in aqueous solutions in response to the addition of a variety of species, including ionic surfactants, salts, and oppositely charged linear polyelectrolytes.[23-28] For example, Müller et al. reported that a cationic brush polymer underwent worm-to-globule-worm shape transitions in dilute aqueous solutions with the sequential addition of sodium dodecyl sulfate (SDS) and β-cyclodextrin (β-CD) due to the complexation of the brushes with SDS and the formation of an inclusion complex between β-CD and SDS.[24] However, even at rather low concentrations, the charged brushes precipitated out immediately from the solution after the addition of SDS. Interesting helical nanostructures of individual linear polyelectrolyte bottlebrushes were observed in highly dilute aqueous solutions by Schmidt and Müller after the addition of surfactants and multivalent ions, respectively.[25-27] Müller et al. also reported that cationic MBBs changed from wormlike to intermediate pearl-necklace and globular conformations in dilute conditions with the addition of an increasing number of short linear poly(sodium styrenesulfonate) (PSSNa) chains.[28] In contrast, the addition of long PSSNa chains collapsed the brushes into the globular state directly.

In the above examples of stimuli-responsive shape-changing MBBs, the collapsed brushes were unstable in the solutions, which have prevented their use in potential applications. To solve this problem, we and others designed shape-changing MBBs with bicomponent side chains, either binary heterografted MBBs composed of two types of side chains[29-36] or homografted bottlebrushes with diblock copolymer side chains.[37,38] One of the side chain polymers in

heterografted brushes and the outer block in homografted bicomponent MBBs serve as a stabilizer for the collapsed MBBs when the other polymer in the side chains become insoluble in solution upon application of external stimuli.[29-38] Using two different stimuli-responsive polymers as side chains in binary heterografted MBBs, Kent and Zhao demonstrated the attainment of two distinct stable globular states from the same brush polymers under different conditions.[32] Herrera-Alonso et al. showed hydrophobic solute-induced worm-to-sphere morphological transitions of amphiphilic MBBs.[33,34] More recently, we reported chaotropic anion (CA)-induced star-globule shape changes of three-arm star MBBs (SMBs) composed of poly(ethylene oxide) (PEO) and either poly(2-(*N*,*N*-dimethylaminoethyl methacrylate) (PDMAEMA) or poly(2-(*N*,*N*-diethylaminoethyl methacrylate) (PDEAEMA) side chains in acidic aqueous solutions at 25 °C.[36] CAs, such as ClO_4^-, typically have a large size and a relatively low charge density.[39-43] These anions are water-structure breakers, that is, they cause the water molecules surrounding them to be less hydrogen bonded and have a higher entropy than water molecules in the bulk. CAs tend to form tight ion pairs with chaotropic cations in water.[39-42] They also display a high tendency to associate with hydrophobic surfaces and groups in aqueous solution, which is termed the chaotropic effect.[43] Both chaotropic ion pairing and chaotropic effect stem from the release of less hydrogen bonded water molecules from the hydration shells of CAs into bulk water to form stronger water-water interactions (i.e., an enthalpic effect). We found that the addition of super CAs, e.g., $[Fe(CN)_6]^{3-}$, and moderate CAs, such as ClO_4^-, induced star-to-globule shape transitions of SMBs in acidic solutions at 25 °C, while weak CAs such as Br^- and Cl^- only caused small decreases in the hydrodynamic sizes (D_h) of SMBs.[36]

Since chaotropic ion pairing and chaotropic effect arise from an enthalpic effect, it is possible to break apart the association by heating. Plamper et al. and Zhang et al. reported that adding small

amounts of large multivalent anions such as $[Co(CN)_6]^{3-}$, $[Fe(CN)_6]^{4-}$, $[Fe(CN)_6]^{3-}$, and $[Cr(CN)_6]^{3-}$ into acidic or near-neutral aqueous solutions of PDMAEMA induced upper critical solution temperature (UCST) behavior in the presence of 0.1 M NaCl.[44,45] Using in situ ATR-FTIR spectroscopy, Fleming et al. observed the wavenumber shifts of the C≡N stretching vibration band of $[Fe(CN)_6]^{3-}$ when paired with protonated PDMAEMA brushes grafted on silicon wafers and the intensity changes upon heating,[46] confirming the ion pairing mechanism for the UCST behavior. Moreover, quaternized PDMAEMA polymers have been reported to exhibit UCST behavior in the presence of specific ions, such as BF_4^- or bis(trifluoromethane)sulfonamide and $CF_3SO_3^-$.[47,48]

On the basis of these reports, we hypothesized that heating might be able to unfold the CA-collapsed globular SMBs with protonated tertiary amine-containing side chains in acidic water to an extended star shape. In the present work, we examined the effects of temperature on CA-collapsed SMB-11, with PEO and PDMAEMA side chains, and SMB-22, with PEO and PDEAEMA side chains, in pH 4.50 water (Scheme 1). Both brush polymers were made by grafting two alkyne-end-functionalized side chain polymers onto an azide-bearing three-arm star backbone polymer using the copper(I)-catalyzed alkyne-azide cycloaddition (CuAAC) reaction.[29-34,36,37,49-51] Six anions were investigated for their effects on the conformations of SMB-11 and -22: super chaotropic $[Fe(CN)_6]^{3-}$ and $[Fe(CN)_6]^{4-}$, moderate chaotropic PF_6^- and ClO_4^-, weak chaotropic I^-, and for comparison, kosmotropic SO_4^{2-}.[43] We found that while super CA-collapsed SMB-11 and -22 remained in the globule state in pH 4.50 water upon heating to 70 °C, moderate CA-collapsed brushes exhibited thermally-triggered globule-to-star shape transitions. In contrast, I^- and SO_4^{2-} had little effects on the conformations of both brush polymers in the studied salt concentration and temperature ranges.

Scheme 1. Synthesis and Behavior in Acidic Water of Three-Arm Star Molecular Bottlebrushes (SMBs) Composed of PEO and Poly(*N*,*N*-dimethylaminoethyl methacrylate) (PDMAEMA) (SMB-11) or Poly(*N*,*N*-diethylaminoethyl methacrylate) (PDEAEMA) Side Chains (SMB-22)

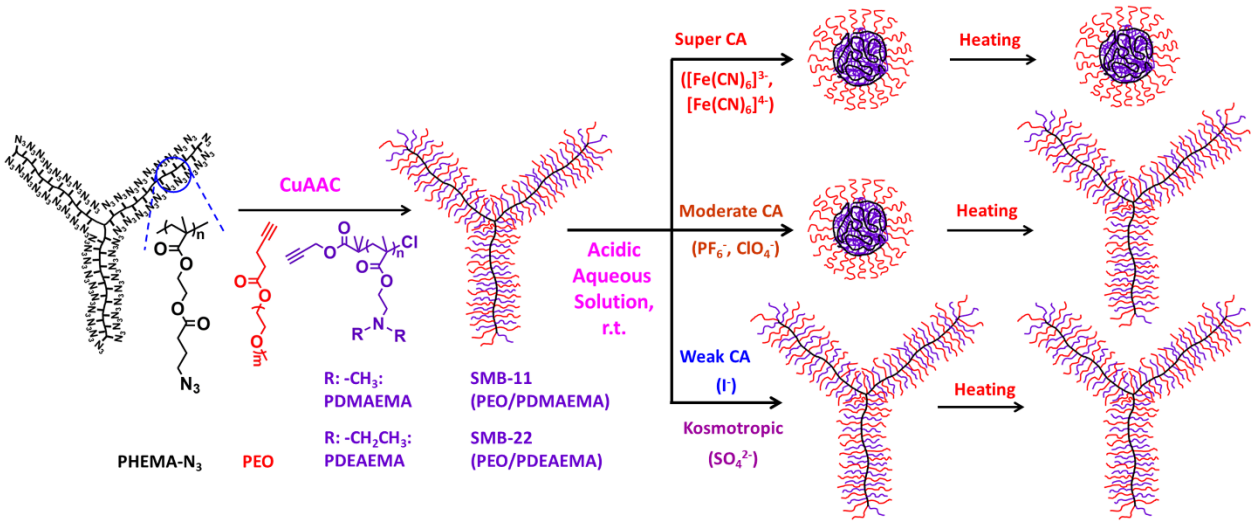

Results and Discussion

Synthesis of SMB-11 and SMB-22. Three-arm star-shaped SMB-11, composed of PEO and PDMAEMA side chains, and SMB-22, comprising PEO and PDEAEMA side chains, were prepared using a method reported previously.[32,36] The details can be found in the Experimental Section in the Electronic Supplementary Information (ESI). Briefly, two alkyne-end-functionalized polymers, PEO with a molecular weight of 5 kDa and either PDMAEMA with a degree of polymerization (DP) of 56 (for SMB-11), or PDEAEMA with a DP of 53 (for SMB-22), were grafted concurrently onto an azide-bearing three-arm star backbone polymer, PHEMA-N_3, using the CuAAC click reaction (Scheme 1). The star backbone PHEMA-N_3, with a DP of 434 per arm, was synthesized through a multi-step process that started with ATRP from a trifunctional initiator followed by a series of post-polymerization reactions to install azide functional groups as described before.[32] Alkyne-end-functionalized PEO was prepared by an esterification reaction between the hydroxyl chain end of poly(ethylene oxide) monomethyl ether with a molecular weight of 5000 Da and 4-pentynoic acid using *N*-(3-dimethylaminopropyl)-*N*′-ethylcarbodiimide

hydrochloride and 4-(dimethylamino)pyridine as the catalysts.[29] Alkyne end-functionalized PDMAEMA and PDEAEMA were made by ATRP of corresponding tertiary amine methacrylate monomers in anisole at 50 °C using propargyl 2-bromoisobutyrate as the initiator. From size exclusion chromatography (SEC) analysis, the dispersities of both alkyne-end-functionalized polymethacrylates were ≤ 1.25 (Figures S1 and S2 in the ESI), indicating that the polymerizations were controlled. The DPs of PDMAEMA and PDEAEMA, 56 and 53, respectively, were calculated from the monomer conversions, determined by ^{1}H NMR spectroscopy analysis, and the monomer-to-initiator feed ratios.

The click reactions for the synthesis of SMB-11 and SMB-22 were performed in THF in 20 mL scintillation vials at ambient temperature under a nitrogen atmosphere. For both brush polymers, slightly excess alkyne-end-functionalized polymers were used with respect to the azide groups on star backbone polymer PHEMA-N_3 in order to achieve a high grafting density. Propargyl benzyl ether was added into the mixtures in the later stage of the click reactions to cap possible remaining unreacted azide moieties on the backbone. To purify the bottlebrush polymers, the copper catalyst was first removed from the reaction mixtures by passing through a basic alumina/silica gel column. The unreacted side chain polymers were removed by multiple rounds of centrifugal filtration of the reaction mixtures at 5000 rpm using 50 kDa MWCO centrifugal filters with a mixture of water and ethanol (50/50, v/v) as the solvent, as confirmed by SEC analysis (Figure S3). ^{1}H NMR analysis of the purified brushes showed that SMB-11 was composed of 43.7% PDMAEMA and 56.3% PEO side chains and SMB-22 contained 41.8% PDEAEMA and 58.2% PEO side chains (Figure S4A and S5A). The calculated grafting densities of SMB-11 and -22 were 86.7% and 83.9%, obtained by using the SEC peak area fractions of the molecular bottlebrushes and the remaining side chain polymers in the SEC traces of the final reaction

mixtures, the feed ratios, and the side chain composition of the purified bottlebrushes (see the ESI). Using a SEC-MALS system equipped with a RI detector and a two-angle light scattering detector, the experimental absolute molecular weights ($M_{w,expt}$) of SMB-11 and -22 were measured to be 9.49×10^6 Da and 9.77×10^6 Da, respectively (Figures S4B and S5B). These values were close to the calculated M_w ($M_{w,cal}$) values, 9.31×10^6 Da for SMB-11 and 9.17×10^6 Da for SMB-22, which were obtained by using the actual M_w values ($M_n \times Đ$) of the backbone and the two side chain polymers, the grafting densities, and the side chain compositions from ^{1}H NMR analysis (see the ESI). The characterization data for star backbone PHEMA-N_3, alkyne-end-functionalized PEO, PDMAEMA, and PDEAEMA, SMB-11, and SMB-22 are summarized in Table 1, along with the side chain compositions, calculated grafting densities, and the $M_{w,cal}$ values of SMB-11 and -22.

Table 1. Characterization Data for Azide-Functionalized Star Backbone PHEMA-N_3, Alkyne End-Functionalized PEO, PDMAEMA and PDEAEMA, SMB-11, and SMB-22

Polymer Sample	DP or Grafting Density (σ)	Molecular Weight and $Đ$
PHEMA-N_3	DP = 434 per arm [a]	$M_{n,SEC} = 2.25 \times 10^5$ Da, $Đ = 1.16$ [d]
PEO	DP = 114 [b]	$M_{n,SEC} = 8.4 \times 10^3$ Da, $Đ = 1.04$ [e]
PDMAEMA	DP = 56 [a]	$M_{n,SEC} = 8.6 \times 10^3$ Da, $Đ = 1.25$ [d]
PDEAEMA	DP = 53 [a]	$M_{n,SEC} = 9.4 \times 10^3$ Da, $Đ = 1.19$ [d]
SMB-11 (PEO/PDMAEMA)	σ = 86.7% [c] (molar ratio: 56.3% : 43.7%)	$M_{w,exp} = 9.49 \times 10^6$ Da [f] $M_{w,cal} = 9.31 \times 10^6$ Da [g]
SMB-2 (PEO/PDEAEMA)	σ = 83.9% [c] (molar ratio: 58.2% : 41.8%)	$M_{w,exp} = 9.77 \times 10^6$ Da [f] $M_{w,cal} = 9.17 \times 10^6$ Da [g]

[a] Degree of polymerization (DP) was calculated from the monomer-to-initiator molar ratio and the monomer conversion (obtained from ^{1}H NMR analysis). [b] The DP of PEO was calculated from the molecular weight of 5000 g/mol provided by the vendor. [c] The value of grafting density (σ) was calculated using the ratio of SEC peak areas of the brushes and the unreacted side chain polymers in the final reaction mixture, the feed ratios of the star backbone to the side chain polymers, and the side chain composition of the purified brushes determined by ^{1}H NMR analysis. [d] $M_{n,SEC}$ and $Đ$ were determined by SEC relative to polystyrene standards using a SEC system with GRAL columns and DMF containing 50 mM LiBr as solvent. [e] $M_{n,SEC}$ and $Đ$ were determined by SEC relative to polystyrene standards using a SEC system with Mixed C columns and THF as solvent. [f] The experimental absolute molecular weight ($M_{w,exp}$) was measured using a SEC-MALS system consisting of a RI detector and a two-angle light scattering detector. [g] The calculated absolute molecular weight ($M_{w,cal}$) was obtained using the actual M_w values of PHEMA-N_3 and the side chain polymers calculated from the DP and the dispersity ($M_n \times Đ$) and the grafting density.

The pK_a values of both PDMAEMA and PDEAEMA in water are around 7.4,[52,53] and thus both polymers are protonated in acidic water. The D_h values of 0.2 mg/g SMB-11 and -22 in acidic water with a pH of 4.50 at 25 °C were found to be very similar to each other, 100.5 and 100.8 nm, respectively (Figure S6). The star shape of the brush polymers can be seen from the AFM height images of the bottlebrush molecules drop cast on bare mica or "Piranha" solution-cleaned glass disks from a 0.050 mg/g solution of SMB-11 in THF and aqueous solutions of 0.050 mg/g SMB-11 and -22 with a pH of 4.50 at room temperature (Figures 1 and S7-S9). For both SMB-11 and -22, most of the brushes shown in the images were three-arm stars, although some molecules appeared to miss one arm, which could be due to the defects in the synthesis of the azide-functionalized star backbone or the mechanical shearing forces during the purification of the brushes and the preparation of AFM samples. Using the ImageJ software, the average arm length and height of SMB-11 from THF were found to be 88.1 ± 26.7 nm (from measurements of 288 arms of three-arm brushes) and 1.5 ± 0.3 nm (from 200 arms). In the pH 4.50 water, the PDMAEMA side chains were protonated; image analysis showed that the average arm length of SMB-11 on glass disks from 207 arms was slightly larger, 98.1 ± 28.2 nm, which could be attributed to the electrostatic repulsive forces between the protonated PDMAEMA side chains, and the average height from the measurements of 200 arms was similar, 1.3 ± 0.3 nm. For SMB-22 from acidic water, the average arm length and height were 95.0 ± 29.0 nm (from 120 arms of three-arm star brushes) and 1.7 ± 0.4 nm (from 200 arms). The maximum length of an arm with a DP of 434 is 110.2 nm, which means that the brushes were highly stretched on the substrates, with degrees of stretching of 89% and 86% for SMB-11 and -22, respectively, on glass disks from pH 4.50 acidic water and 80% for SMB-11 from THF. The high stretching could be partially caused by the strong electrostatic interactions with the substrates.

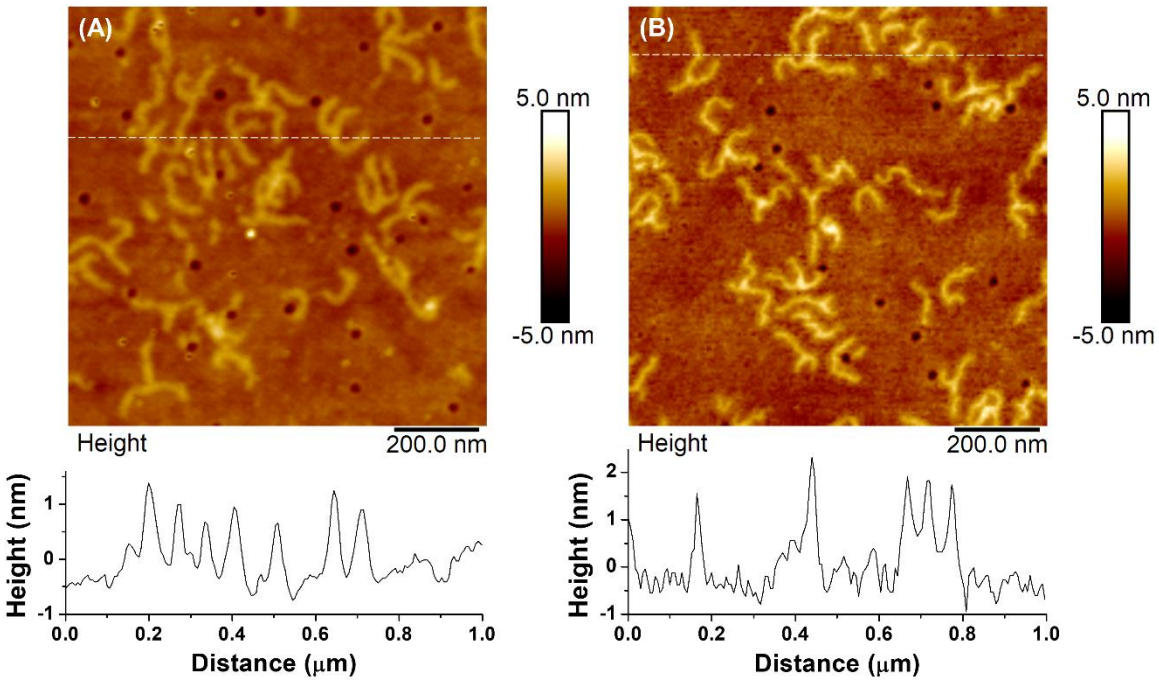

Figure 1. AFM height images (1 × 1 μm) of SMB-11 (A) and SMB-22 (B) drop cast on glass disks from 0.050 mg/g brush polymer solutions in pH 4.50 water at room temperature, with a cross-sectional profile along the dashed line in each image.

Dynamic Light Scattering (DLS) Study of the Effects of Various Salts on Conformations of SMB-11 and -22 in pH 4.50 Water at 25 °C. Chaotropic ion pairing and chaotropic effect, which have recently emerged as a generic driving force for supramolecular assmbly,[43,54,55] provide new opportunities to control conformations and trigger shape transitions of polyelectrolyte MBBs in aqueous solutions. We previously investigated the effects of six CAs (Cl^-, Br^-, SCN^-, ClO_4^-, $Fe(CN)_6^{3-}$, and $S_2O_8^{2-}$) on the conformations of similar PEO/PDMAEMA and PEO/PDEAEMA star MBBs in acidic aqueous solutions at 25 °C with increasing anion concentration.[36] Among the six anions, Cl^- and Br^- are weak CAs, exerting negligible effects on brush conformation in pH 4.00 water, while $Fe(CN)_6^{3-}$ and $S_2O_8^{2-}$ are super CAs,[43] which collapsed protonated star brushes at concentrations less than 1 mM for 0.1 mg/g SMBs. On the other hand, SCN^- and ClO_4^- are moderate CAs, which showed an ability to collapse PEO/PDEAEMA star brushes into globules at concentrations of tens to hundreds mM. These observations are consistent with the chaotropicity

scale proposed by Marcus based on the ion hydration parameters: $Cl^- < Br^- < SCN^- < ClO_4^- << S_2O_8^{2-} \sim [Fe(CN)_6]^{3-}$,[36,43] where Cl^-, Br^-, SCN^-, and ClO_4^- caused an effective loss of 1.01 – 1.27 hydrogen bonds in the solvation shell around the ion, and $S_2O_8^{2-}$ and $Fe(CN)_6^{3-}$ brought about a loss of ~ 2 hydrogen bonds in the surrounding hydration layer.[43]

In the present work, we first studied the effects of five CAs from the following salts, $Na_4[Fe(CN)_6]$, $K_3[Fe(CN)_6]$, $NaPF_6$, $NaClO_4$, and NaI, and kosmotropic SO_4^{2-} from Na_2SO_4 on the conformations of SMB-11 and -22 at 25 °C and then examined the effects of temperature. Aqueous solutions of 0.2 mg/g SMB-11 and -22 in pH 4.50 acidic water were prepared, and for each CA, the salt concentration was gradually increased. $[Fe(CN)_6]^{3-}$ is known to be a super CA with an effective loss of 2.01 hydrogen bonds in the solvation shell around the anion in water.[43] From the literature, $[Fe(CN)_6]^{4-}$ appears to be a super CA with a water structure breaking ability similar to $[Fe(CN)_6]^{3-}$.[44,45] $S_2O_8^{2-}$ was not selected here because $K_2S_2O_8$ is a redox radical initiator.[56,57] PF_6^- and ClO_4^- are moderate CAs, causing a loss of 1.43 and 1.27 hydrogen bonds in the solvation shell of the anion, respectively.[43] According to Assaf and Nau, there is a loss of 1.37 hydrogen bonds in the hydration layer around I^-,[43] which places I^- in between ClO_4^- and PF_6^- in the water-structure breaking ability. However, the experimental results from Gao et al. in the study of CA-induced micellization of PEO-*b*-PDEAEMA in acidic aqueous solutions showed that I^- was actually a weaker CA than ClO_4^-.[54] On the other hand, SO_4^{2-} is a kosmotropic anion, which increases water structuring in the solvation shell with a gain of 0.78 hydrogen bonds,[43] and is used here for comparison with various CAs. K^+ is a weakly structure-breaking cation, while Na^+ is a borderline ion;[40] these two cations are often listed side by side in the Hoffmeister series, and thus we believe that their effects on the conformation of SMBs should be very similar to each other and the effects observed here should be from the anions of the salts. According to Marcus, NH_4^+,

$CH_3NH_3^+$, and $N^+(CH_3)_4$ are chaotropic cations, while $N^+(CH_2CH_3)_4$ is a borderline ion between water-structure making and breaking.[40] Thus, on the basis of this trend, it is very likely that the protonated monomer units of PDMAEMA and PDEAEMA in acidic water are chaotropic cations.

Figure 2 shows the plots of the D_h of 0.2 mg/g SMB-11 and -22 in pH 4.50 water at 25 °C as a function of increasing salt concentration for the six salts from DLS measurements. Note that as mentioned earlier PDMAEMA and PDEAEMA exhibit similar pK_a values of ~ 7.4 in water,[52,53] although the lengths of two alkyl substituents at the nitrogen atom are different. Thus, at pH = 4.50, the tertiary amine groups in both brush polymers were fully protonated. The D_h values of SMB-11 and -22 in the presence of a salt with a concentration of 0.01 mM were very similar, ~ 97 nm, regardless of the types of the salts. Upon increasing the concentrations of the salts, the two brush polymers responded similarly to the same salt (i.e., the same anion). For $[Fe(CN)_6]^{4-}$ and $[Fe(CN)_6]^{3-}$, the hydrodynamic sizes of both SMB-11 and -22 decreased sharply to ~ 67 nm in the salt concentration range of 0.10 – 0.30 mM, while single, narrow size distributions were maintained (Figures S10 and S11). Although $[Fe(CN)_6]^{4-}$ appeared to be more efficient in collapsing SMB-11 than $[Fe(CN)_6]^{3-}$, both anions performed very similarly in inducing the size changes of SMB-22. These observations indicated that $[Fe(CN)_6]^{4-}$ is a super CA as expected, with a similar water-structure breaking ability to $[Fe(CN)_6]^{3-}$. Although there appeared to be no difference in the salt concentration for the collapse of both brush polymers by $[Fe(CN)_6]^{4-}$, the full collapse of SMB-22 by $[Fe(CN)_6]^{3-}$ occurred at a slightly lower concentration (0.12 mM for SMB-22 versus 0.25 mM for SMB-11).

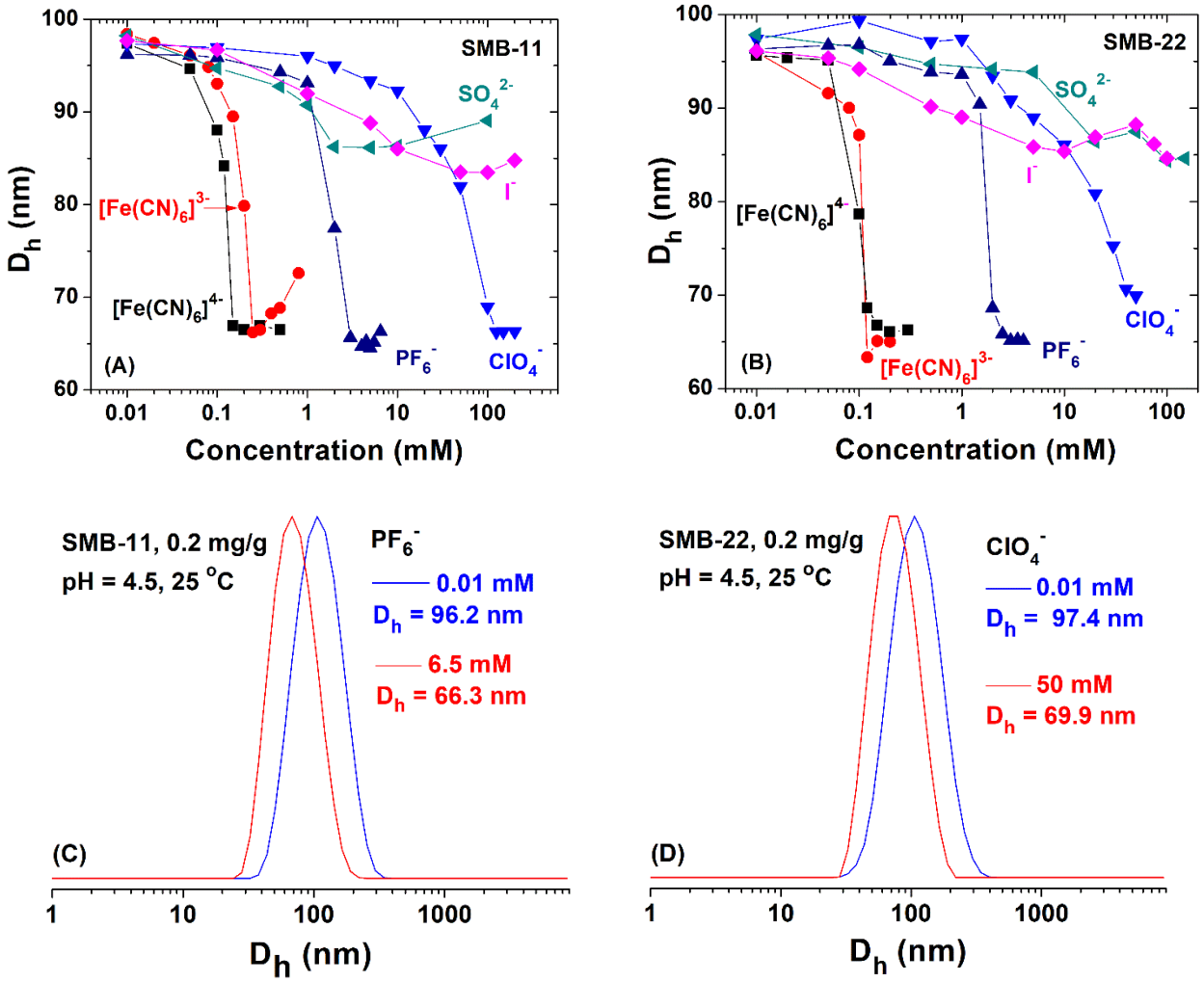

Figure 2. Apparent hydrodynamic diameter (D_h) at 25 °C of 0.2 mg/g SMB-11 (A) and SMB-22 (B) in pH 4.50 water as a function of increasing concentration of a salt from DLS measurements for $Na_4[Fe(CN)_6]$ (black square), $K_3[Fe(CN)_6]$ (red circle), $NaPF_6$ (navy up-pointing triangle), $NaClO_4$ (blue down-pointing triangle), NaI (magenta rhombus), and Na_2SO_4 (dark cyan left-pointing triangle). (C) and (D) Hydrodynamic size distributions of SMB-11 in the presence of 0.01 and 6.5 mM PF_6^- and SMB-22 in the presence of 0.01 and 50 mM ClO_4^-.

For PF_6^-, the sharp size reduction transitions of both brush polymers occurred in the concentration range of 1 – 3 mM, which was about one order in magnitude higher than those for the two super CAs. For ClO_4^-, the size transition was somewhat broader and occurred at even higher concentrations than PF_6^-; the full collapse was observed at 125 mM with a D_h of 66.3 nm for SMB-11 and at 50 mM with a D_h of 69.9 nm for SMB-22. Both PF_6^- and ClO_4^- appeared to be more efficient in collapsing SMB-22 than SMB-11 as evidenced by the lower concentrations for

the full collapse of SMB-22. We stress here that all the data points in Figure 2A and B correspond to single size distributions with representative examples shown in Figure 2C and D (as well as Figures S10 and S11). In contrast, the addition of I^- and SO_4^{2-} did not produce sharp size decreases but small variations for both brush polymers, indicating no dramatic conformational changes in the studied salt concentration ranges. It should be noted here that for $[Fe(CN)_6]^{3-}$, PF_6^-, I^-, and SO_4^{2-}, after reaching the minimum value, the D_h of SMB-11 exhibited a slight increase with the further increase of the salt concentration (Figure 2A). A small upturn was also observed for the D_h of SMB-22 with increasing concentration of $[Fe(CN)_6]^{3-}$, I^-, and SO_4^{2-} (Figure 2B), although the latter two seemed to show even more complicated behavior. The observed slight rise of the hydrodynamic diameter of the collapsed star brushes with the increase of the concentration of the aforementioned anions is in line with the literature reports on the widely studied re-entrant behavior of polyelectrolyte chains induced by multivalent ions (i.e., the charged polymer chains first undergo conformational contraction or collapse and then re-expansion with increasing the concentration of a multivalent ion).[58-60] This behavior is commonly attributed to the condensation of multivalent ions on charged polymer chains and the overcompensation of the charges in the intermediate salt concentration region, resulting in charge inversion and consequently re-swelling. A similar re-entrant behavior was also reported for sodium polystyrene sulfonate with the addition of monovalent Cs^+,[60] for which the reason was unclear. The observed upturn of the D_h in Figure 2 might plateau at higher salt concentrations. For other anions shown in Figure 2, there was essentially no change in the D_h of the brushes after the full collapse; it is possible that the D_h could rise slightly if the salt concentration is further increased. However, the DLS experiments likely will be complicated by the appearance of large species at higher ion concentrations as we observed before for the star brushes.[36]

Our observations for the effects of ClO_4^- and I^- on the hydrodynamic diameters of SMB-11 and -22 were in accordance with their abilities in inducing the micellization of PEO-*b*-PDMAEMA and PEO-*b*-PDEAEMA reported by Gao et al.[52] The observed effect of kosmotropic anion SO_4^2 in the studied concentration range indicated that the collapse of the brushes induced by $[Fe(CN)_6]^{4-}$ and $[Fe(CN)_6]^{3-}$ was from their chaotropicity, although their charges, 4- and 3-, might also contribute to their efficiency in collapsing the star brushes. We note here that Xu et al. observed by AFM that homografted poly(methacryloylethyl trimethylamine iodide) MBBs formed helical and spherical nanostructures in very dilute aqueous solutions after the addition of di- and trivalent anions,[27] which was ascribed to the multivalency of the ions. Clearly, super CAs caused larger and sharper decreases in the D_h values of SMB-11 and -22 at lower concentrations, while moderate CAs collapsed the brushes at higher concentrations and weak CA I^- and kosmotropic anion SO_4^{2-} produced small variations of the D_h for both brush polymers. These results are in line with our previous report.[36]

Effects of Temperature on Shape Transitions of Star Brushes SMB-11 and -22 Induced by Super CAs, $[Fe(CN)_6]^{4-}$- and $[Fe(CN)_6]^{3-}$. Figure 3 shows the plots of D_h of 0.2 mg/g SMB-11 in pH 4.50 water in the presence of 0.25, 0.50, and 0.80 mM $[Fe(CN)_6]^{3-}$ and 0.20 mg/g SMB-22 in the presence of 0.20 mM $[Fe(CN)_6]^{4-}$ as a function of temperature in the typical temperature range of 20 to 70 °C. The plot of the D_h of 0.20 mg/g SMB-22 in pH 4.50 water with the addition of 0.12 mM $[Fe(CN)_6]^{3-}$ versus temperature in the same temperature range can be found in the ESI (Figure S12). For all the five solutions, temperature had little effect on the hydrodynamic sizes of both brush polymers in the temperature range of 20 to 70 °C and no large and sharp size changes were observed while maintaining a single size distribution (Figures S13 and S14), suggesting that the bottlebrush molecules remained in the collapsed globular state even at 70 °C. Note that Plamper

et al. reported a UCST of ~ 24 °C for 0.1 mg/mL PDMAEMA with a DP of 100 at pH = 5.0 in the presence of 1.2 mM $[Co(CN)_6]^{3-}$ and 0.1 N NaCl and stated that $[Fe(CN)_6]^{4-}$ showed a similar effect.[44] In contrast, Zhang et al. reported a UCST of ~ 60 °C for 0.5 mg/mL PDMAEMA with a DP of 64 at pH = 5.0 in the presence of 8 mM $[Fe(CN)_6]^{3-}$ and 0.1 M NaCl.[45] Although we cannot compare our star bottlebrushes directly with linear polymers because of the much higher local density of protonated tertiary amine groups and it is totally possible that the UCST transition temperature for our brush systems could be higher than 70 °C, we note here that in those two reports 0.1 M NaCl was added to moderate the electrostatic interactions between the protonated tertiary amine groups and complex metal anions. Plamper et al. emphasized that the effects were only observed in buffers containing a considerable amount of NaCl (~ 0.1 M NaCl) and no UCST was found in the absence of a buffer.[44] Presumably, the chaotropic ion pairing of protonated PDMAEMA with super CAs was so strong that heating could not break apart the ion pairs. Adding a large amount of NaCl could modulate the electrostatic interactions and make the UCST transition appear in a convenient temperature range. For star brushes, as mentioned earlier, the local density of the protonated side chains (and thus protonated tertiary amine groups) is significantly higher, which may also result in a different scenario for chaotropic ion pairing and chaotropic effect. Thus, it is not surprising that no size transitions were observed for the collapsed globular brushes upon heating under our experimental conditions.

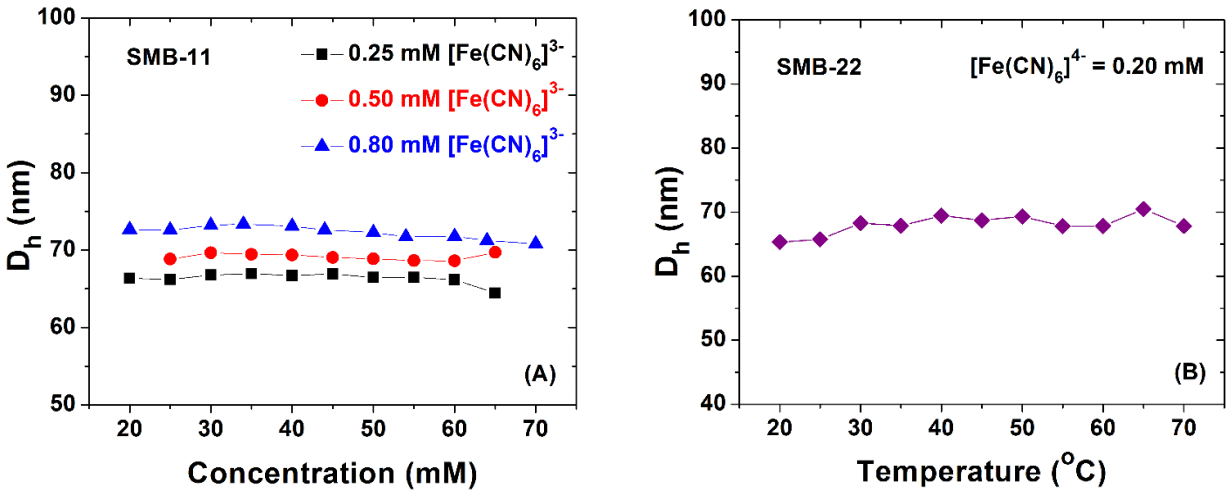

Figure 3. (A) Apparent hydrodynamic size (D_h) of 0.2 mg/g SMB-11 in pH 4.50 water in the presence of 0.25 mM (black square), 0.50 mM (red circle), and 0.80 mM (blue triangle) $K_3[Fe(CN)_6]$ as a function of temperature. (B) D_h of 0.2 mg/g SMB-22 in pH 4.50 water in the presence of 0.20 mM $Na_4[Fe(CN)_6]$ as a function of temperature.

AFM was then used to visualize the brush molecules at different temperatures. A portion of the DLS sample with 0.20 mg/g SMB-11 in the presence of 0.3 mM $K_3[Fe(CN)_6]$ (Figure 2A) was diluted with pH 4.50 water at ambient conditions to 0.050 mg/g SMB-11 with 0.075 mM $K_3[Fe(CN)_6]$ for the preparation of AFM samples. The diluted solution was drop cast on "Piranha"-cleaned glass disks at room temperature (20 °C) and in a 70 °C oven, which were imaged by AFM at ambient conditions. Figure 4 shows the AFM height images at 20 and 70 °C, respectively, and more images can be found in the ESI (Figures S15 and S16). Evidently, SMB-11 brush molecules were collapsed and overall globular at both 20 and 70 °C, unlike the star-shaped molecules seen in Figure 1A. In Figure 4A, one brush molecule with three tightly associated lobes from collapsed arms, as indicated by three arrows, can be clearly seen. Despite the globular state of SMB-11 observed at both 20 and 70 °C, there are still some noticeable differences. From the cross-sectional profiles, the brush molecules in Figure 4A are generally taller than those in Figure 4B. Image analysis using the ImageJ software shows that the average height is 10.6 ± 2.4 nm (from measurements of 100 brushes) at 20 °C and 7.0 ± 1.9 nm at 70 °C (from 200 globules). In addition,

the brush molecules in Figure 4B appear to be flattened to some degree, likely caused by the high temperature that might soften the collapsed globular brushes. The average size of the brushes was 46.3 ± 9.0 nm at 20 °C (from measurements of 109 globules) and 49.4 ± 9.2 nm at 70 °C (from measurements of 200 globular nanoobjects).

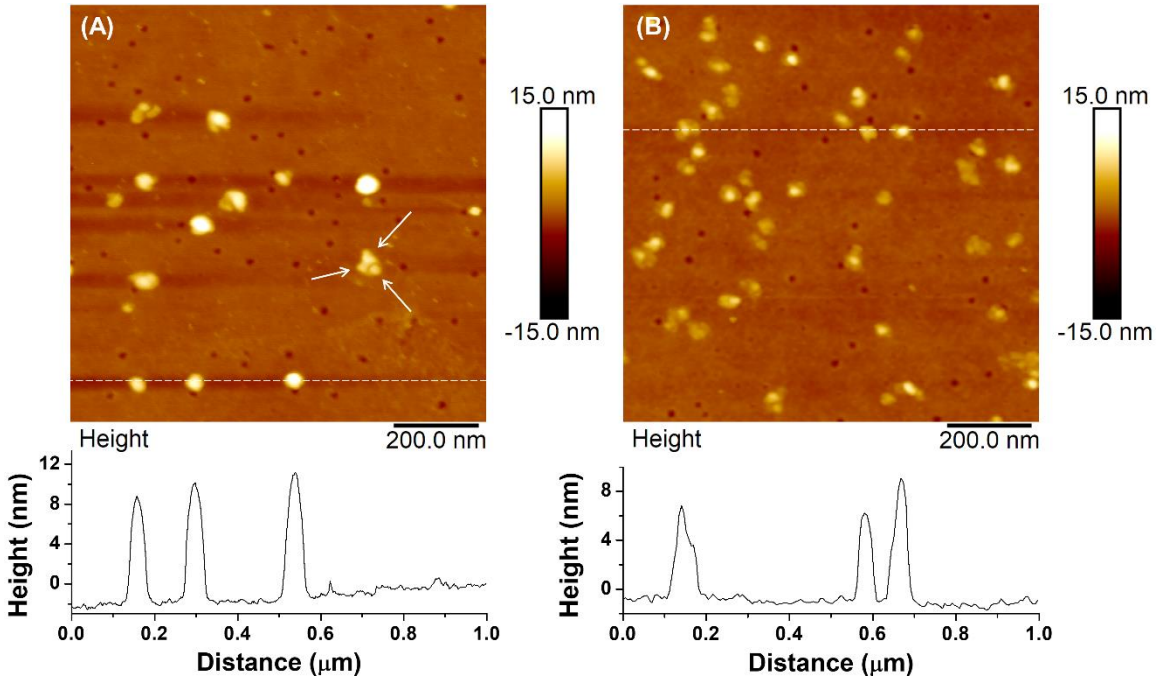

Figure 4. AFM height images (1 × 1 μm) of SMB-11 drop cast on glass disks at 20 °C (A) and 70 °C (B) from a 0.050 mg/g SMB-11 solution in pH 4.50 water in the presence of 0.075 mM $K_3[Fe(CN)_6]$, with a cross-sectional profile along the dashed line in each image. The solution used to prepare AFM samples was diluted from a 0.2 mg/g solution of SMB-11 in pH 4.50 water with 0.30 mM $K_3[Fe(CN)_6]$ using pH 4.50 acidic water.

Effects of Temperature on Shape Transition of Star Brushes SMB-11 and -22 Induced by Moderate CAs, PF_6^- and ClO_4^-. Figure 5 shows the DLS data for SMB-11 and -22 in pH 4.50 water with the addition of $NaPF_6$ at various temperatures. For SMB-11 in the presence of 4.0 mM $NaPF_6$, the D_h was ~ 65 nm in the temperature range of 5 – 30 °C (Figure 5A). Upon further heating from 30 to 40 °C, the D_h increased sharply from 67.2 nm to 93.6 nm, respectively, with a transition middle point at 35 °C. Above 40 °C, the D_h showed only small changes; at 70 °C the apparent

diameter was 97.3 nm, which is almost the same as that observed in the presence of 0.01 mM $NaPF_6$ at 25 °C (96.2 nm, Figure 2A), suggesting that the brushes underwent a thermally-induced globule-to-star shape transition. Note that throughout the heating process during the DLS measurements, a single size distribution was maintained; the distributions for 5 and 70 °C are shown in Figure 5B as examples.

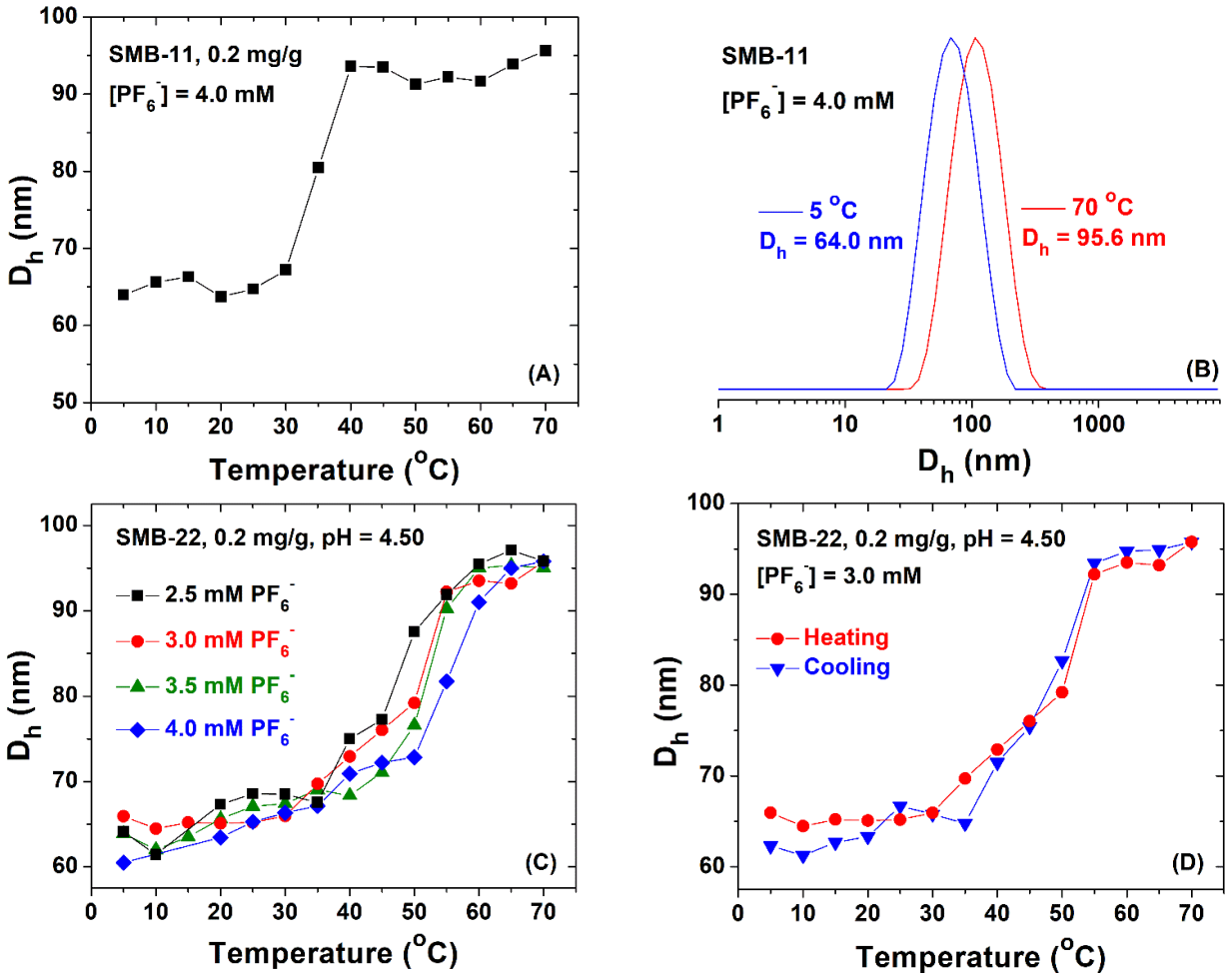

Figure 5. DLS studies of SMB-11 and SMB-22 in pH 4.50 water in the presence of $NaPF_6$. (A) Apparent hydrodynamic size (D_h) of 0.2 mg/g SMB-11 in pH 4.50 water with 4.0 mM $NaPF_6$ as a function of temperature. (B) Hydrodynamic size distributions of 0.2 mg/g SMB-11 in pH 4.50 water with 4.0 mM $NaPF_6$ at 5 and 70 °C. (C) Plots of D_h of 0.2 mg/g SMB-22 in pH 4.50 water in the presence of 2.5, 3.0, 3.5, and 4.0 mM $NaPF_6$ versus temperature upon heating. (D) Plot of D_h of 0.2 mg/g SMB-22 in pH 4.50 water with 3.0 mM $NaPF_6$ versus temperature from heating and cooling processes. All data points correspond to a single distribution (Figure S17).

Comparable size transitions were observed for SMB-22 in pH 4.50 water in the presence of 2.5, 3.0, 3.5, and 4.0 mM $NaPF_6$, with the D_h increasing from ~ 65 nm at 20 °C to ~ 95 nm at 70 °C (Figure 5C). There appeared to be a general trend that the transition temperature increased with increasing concentration of $NaPF_6$ from 2.5 to 4.0 mM, which is reasonable considering that the ion pairing is a dynamic equilibrium between paired ions and free ions. A larger concentration of PF_6^- would suppress the dissociation and thus a higher temperature is needed to unfold the brushes to the starlike state. The size transition was reversible, as shown in Figure 5D by the plots of D_h of 0.2 mg/g SMB-22 with 3.0 mM $NaPF_6$ versus temperature from a heating-cooling cycle.

Similar to the brushes collapsed by PF_6^-, both ClO_4^--collapsed brush polymers in acidic water exhibited thermally-induced size transitions (Figure 6). Upon heating from 20 to 70 °C, the D_h of SMB-11 in the presence of 125, 150, and 200 mM $NaClO_4$ increased substantially, from ~ 65 nm at 20 °C to ~ 85 nm at 70 °C, with the transitions occurring in the temperature range of 30 to 45 °C (Figure 6A), and the size transitions were reversible as shown in Figure 6B for the brushes with 125 mM $NaClO_4$. Much like the observation for the transitions of SMB-22 in the presence of different concentrations of $NaPF_6$, the transition temperature was higher for a higher $NaClO_4$ concentration. However, the D_h values at 70 °C (~ 85 nm) were noticeably smaller than that of SMB-11 in the presence of 0.01 mM ClO_4^- at 25 °C (~ 97 nm in Figure 2A) and that in the presence of 4.0 mM $NaPF_6$ at 70 °C (95.6 nm in Figure 5A), which could be caused by the higher $NaClO_4$ concentrations that screened the electrostatic repulsive interactions at higher temperatures. SMB-22 in the presence of 50 mM $NaClO_4$ also underwent a size transition upon heating (Figure 6C). These data suggest that SMB-11 and -22 collapsed by moderate CAs can undergo thermally-induced reversible globule-to-star transitions.

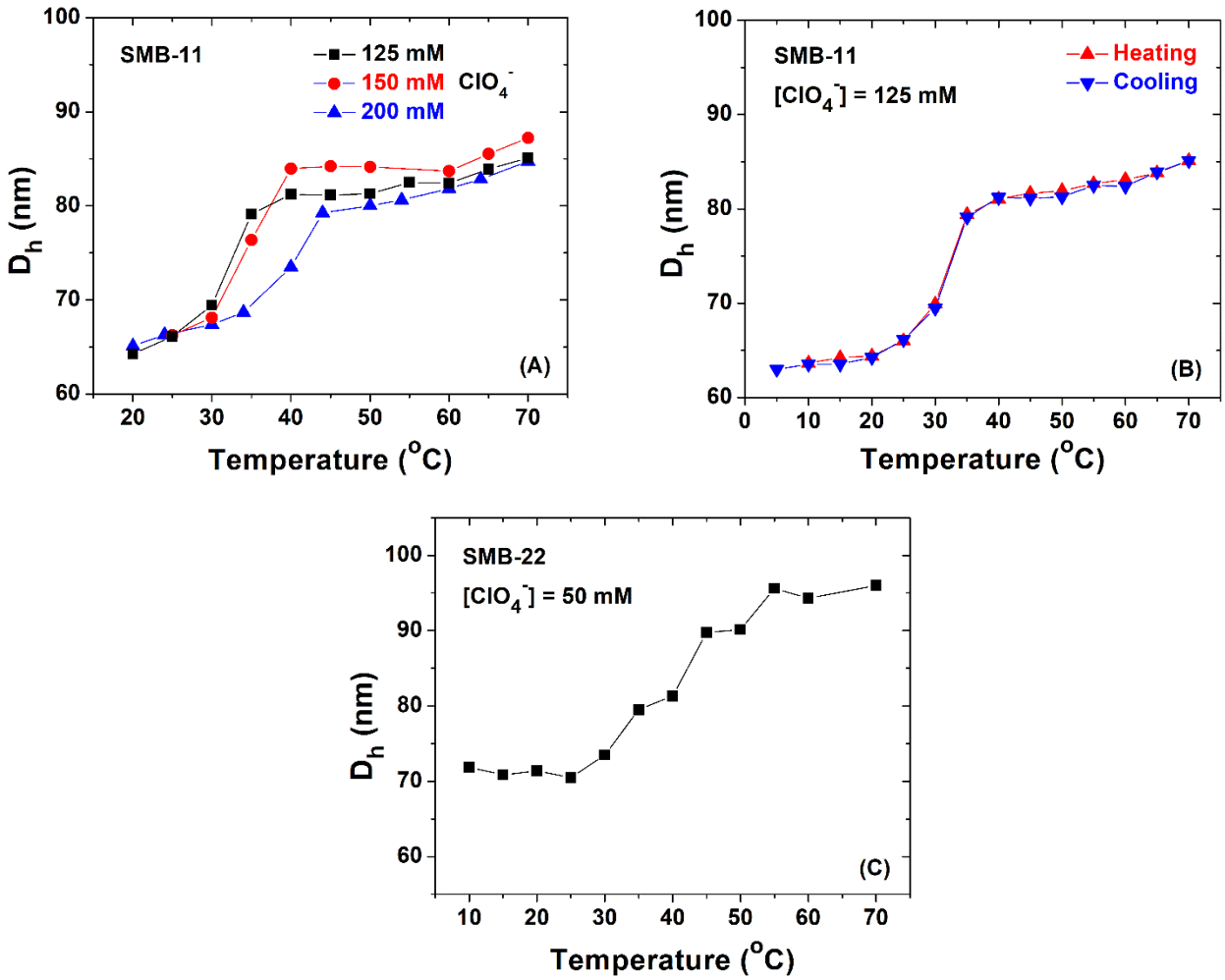

Figure 6. (A) Plots of apparent hydrodynamic size (D_h) of 0.2 mg/g SMB-11 in pH 4.50 water in the presence of 125 mM (black square), 150 mM (red circle), and 200 mM (blue triangle) $NaClO_4$ versus temperature. (B) Plot of D_h of 0.2 mg/g SMB-11 in pH 4.50 water with 125 mM $NaClO_4$ versus from a heating and cooling cycle. (C) Plot of D_h of 0.2 mg/g SMB-22 in pH 4.50 water with 50 mM $NaClO_4$ versus temperature. All data points correspond to a single-size distribution (Figures S18 and S19).

Comparing the thermal behavior of SMB-11 and -22 at the same concentration of PF_6^- in Figure 5A and C (4.0 mM), the transition temperature for SMB-22 (~ 55 °C in Figure 5C) is substantially higher than that for SMB-11 (35 °C in Figure 5A). Similarly, even if the $NaClO_4$ concentration was only 50 mM for SMB-22 in Figure 6C, the transition temperature was higher than those of SMB-11 at higher salt concentrations (125 and 150 mM in Figure 6A). These data suggested that the interactions of PF_6^- and ClO_4^- with protonated PDEAEMA were likely stronger than protonated

PDMAEMA, consistent with the observation in Figure 2A that a full collapse of SMB-22 occurred at lower concentrations of PF_6^- and ClO_4^- than SMB-11. As discussed earlier, according to Marcus, $(CH_3)_4N^+$ is chaotropic, while $(C_2H_5)_4N^+$ is on the borderline between chaotropic and kosmotropic cations.[40] On the basis of this, we reason that under the same conditions the protonated tertiary amine groups of PDMAEMA, $-CH_2CH_2N^+H(CH_3)_2$, should be stronger in terms of chaotropicity than those of PDEAEMA, $-CH_2CH_2N^+H(C_2H_5)_2$, which means that the ion pairing of $-CH_2CH_2N^+H(CH_3)_2$ with a moderate CA (either PF_6^- or ClO_4^- here) should be stronger than that between $-CH_2CH_2N^+H(C_2H_5)_2$ and the same CA. However, this cannot explain what we observed here. The stronger effect of the same moderate CA for SMB-22 than SMB-11 very likely comes from the chaotropic effect that chaotropic anions have a high tendency to associate with the more hydrophobic ethyl groups in the tertiary amine pendant groups of PDEAEMA.

AFM was used to visualize the SMB-11 drop cast on glass disks from a solution of 0.050 mg/g SMB-11 in pH 4.50 water with 1.5 mM $NaPF_6$ at 20 and 70 °C (Figures 7, S20 and S21), which was diluted from a 0.2 mg/g solution of the brush polymer in the presence of 6.0 mM $NaPF_6$. At 20 °C, the brush molecules were round in shape on the substrate, but the collapsed arms were not as tight as the globular brushes in Figure 4A and the star backbone can be seen in some molecules. The average size from the measurements of 121 brushes was 63.8 ± 11.3 nm, and the aveage height from 200 globules was found to be 2.9 ± 0.8 nm. In contrast, at 70 °C, extended three-arm star brushes were observed, although some molecules appeared to be broken. Measurements of 156 arms of star brushes showed an average arm length of 95.7 ± 33.4 nm, similar to that of SMB-11 from pH 4.50 water without a salt (98.1 ± 28.2 nm), and the average height of 200 arms of the brushes was 1.5 ± 0.3 nm. We also imaged SMB-22 brushes drop cast on glass (Figures 8, S22 and S23); collapsed globular and ellipsoidal nanoobjects were seen at 0 °C, with an average size

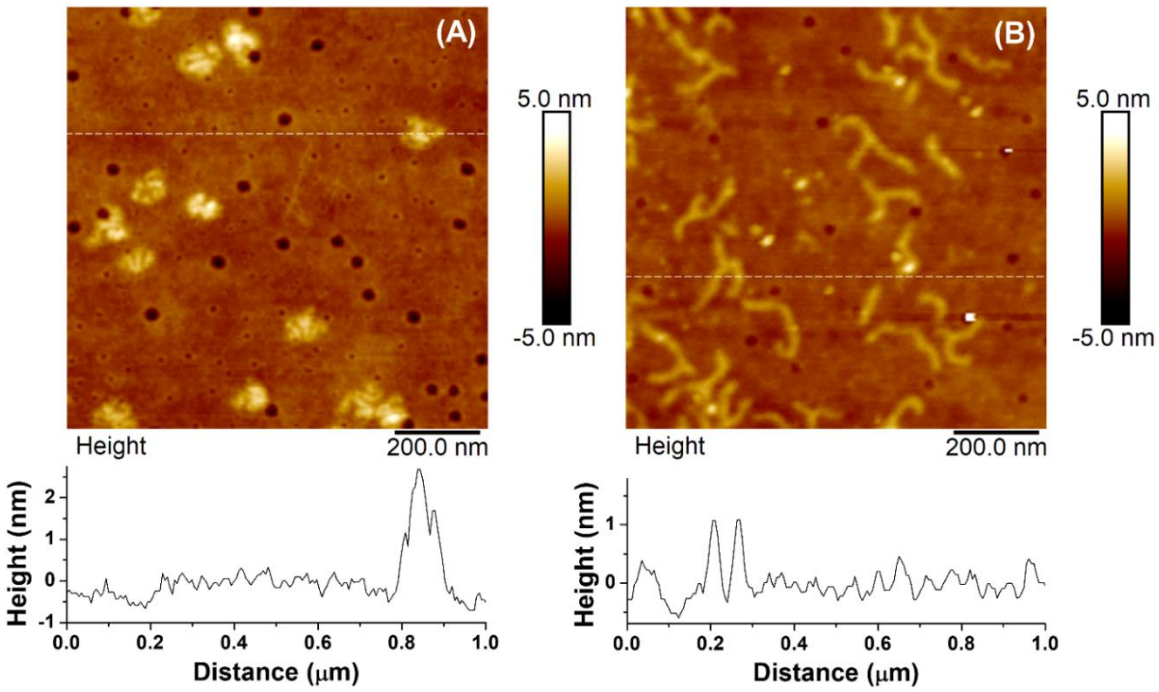

Figure 7. AFM height images (1 × 1 μm) of SMB-11 drop cast on glass disks from a solution of 0.050 mg/g SMB-11 in pH 4.50 water with 1.5 mM $NaPF_6$ at 20 °C (A) and 70 °C (B), with a cross-sectional profile along the dashed line in each image. The solution was diluted from a pH 4.50 solution of 0.2 mg/g SMB-11 with 6 mM $NaPF_6$ using pH 4.50 water.

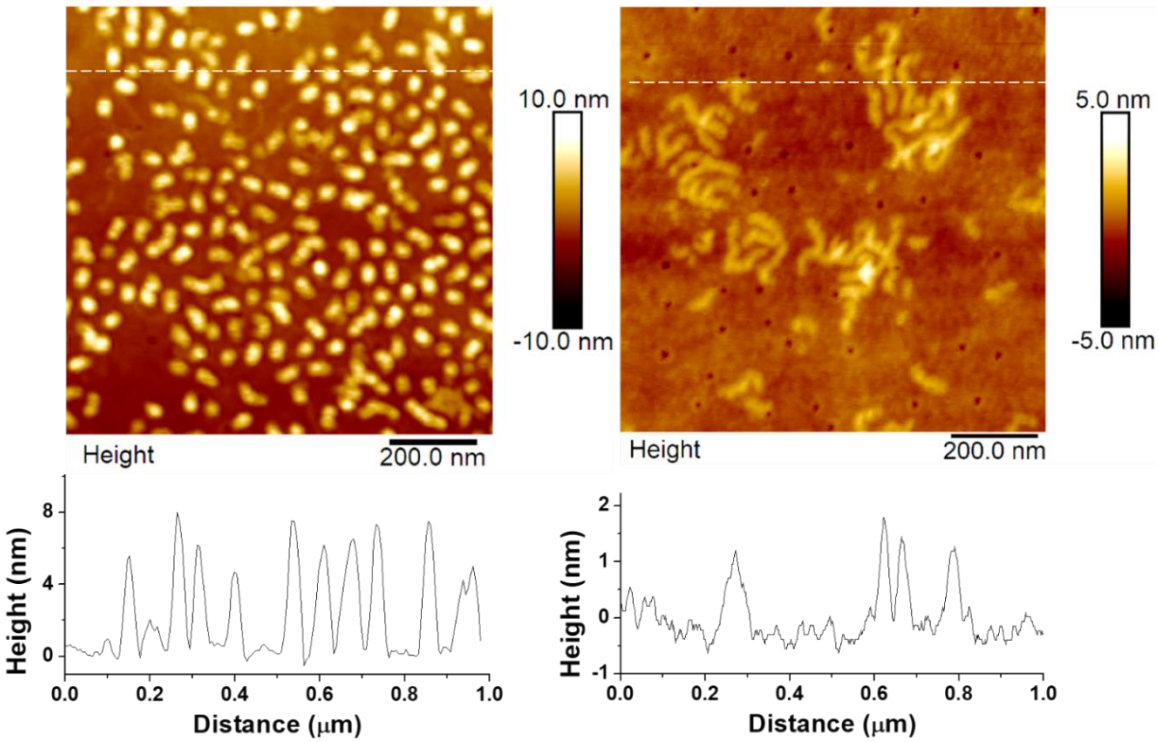

Figure 8. AFM height images of SMB-22 drop cast on a glass disk from a 0.050 mg/g solution of SMB-22 in pH 4.50 water with 1.0 mM $NaPF_6$ at 0 °C (A) and 70 °C (B). The solution was diluted from a pH 4.50 solution of 0.2 mg/g SMB-22 with 4 mM $NaPF_6$ using pH 4.50 water.

of 40.9 ± 7.2 nm (from 300 nanoobjects) and an average height of 6.5 ± 1.4 nm (from 200 molecules). Same as SMB-11 shown in Figure 7B, extended star brush molecules were observed at 70 °C (Figures 8B and S23), with an average height of 1.6 ± 0.3 nm. The average arm length from the measurements of 255 arms of star brushes was 92.6 ± 33.6 nm. These images confirmed the thermally induced globule-to-star shape transitions hinted from DLS studies (Figure 5).

Effects of Temperature on Conformations of Star Brushes SMB-11 and -22 in the Presence of Weak Chaotropic Anion I^- and Kosmotropic Anion SO_4^{2-}. As shown in Figure 2, the addition of weak CA I^- and kosmotropic anion SO_4^{2-} into the aqueous solutions of 0.2 mg/g SMB-11 and -22 with a pH of 4.50 at 25 °C only caused small and gradual size variations, which suggested no star-to-globule shape transition. Figure 9 shows the D_h as a function of temperature from heating processes for 0.2 mg/g SMB-11 in the presence of 50 mM NaI and 0.2 mg/g SMB-22 with 10 mM NaI in pH 4.50 water. For both SMB-11 and SMB-22, the D_h appeared to increase slightly with increasing temperature, but as expected, there were no sharp size transitions. At a lower salt concentration for SMB-22 (10 mM), the size increase was slightly larger than that for SMB-11 at a higher salt concentration (50 mM) upon heating from 20 to 70 °C. Figure 10 shows the plots of D_h of SMB-11 in the presence of 5 mM Na_2SO_4 and SMB-22 with 50 mM Na_2SO_4 versus temperature from heating processes. The D_h values of both brush polymers varied slightly with temperature. Here, however, the size of SMB-11 in the presence of 5 mM Na_2SO_4 showed a small decrease of ~ 3 nm from 15 to 65 °C, whereas the D_h of SMB-22 with 50 mM Na_2SO_4 increased slightly upon heating. Since each SO_4^{2-} has a charge of 2- and can form a bridge between two protonated tertiary amine groups, it is possible that the bridging interactions are weakened at higher temperatures, causing the size to increase slightly with temperature. However, we could not rationalize the small but noticeable decrease in the size of SMB-11 (Figure 10A).

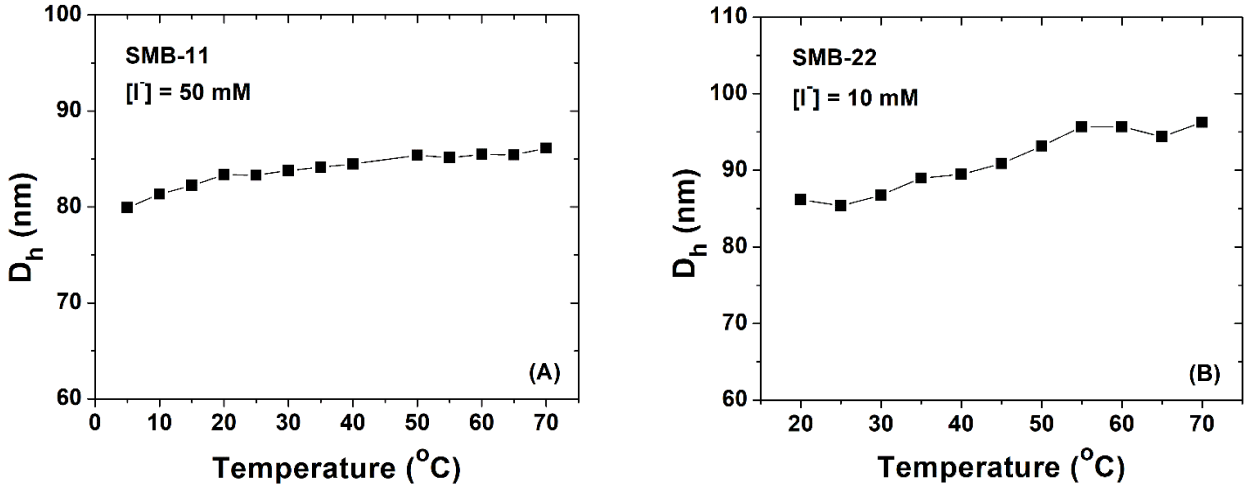

Figure 9. Plots of D_h of (A) 0.2 mg/g SMB-11 in pH 4.50 water in the presence of 50 mM NaI and (B) 0.2 mg/g SMB-22 in pH 4.50 water in the presence of 10 mM NaI versus temperature. All data points correspond to a single hydrodynamic size distribution (Figure S24). (Note that in (A) at 45 °C large species were observed and the data point was not included.)

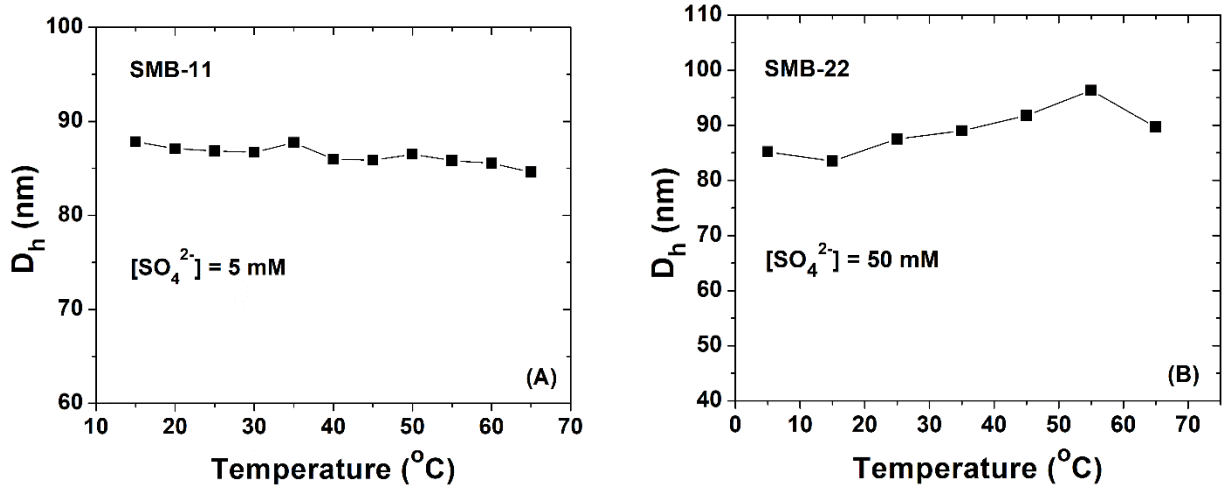

Figure 10. (A) Plots of D_h of (A) 0.2 mg/g SMB-11 in pH 4.50 water with 5 mM Na_2SO_4 and (B) 0.2 mg/g SMB-22 in pH 4.50 water with 50 mM Na_2SO_4 versus temperature. All the data points are single size distributions (Figure S25).

Figures 11, S26, and S27 show the AFM height images of SMB-11 drop cast on glass substrates from a 0.050 mg/g solution with a pH value of 4.50 in the presence 2.5 mM Na_2SO_4 at 20 and 70 °C. The solution for the preparation of AFM samples was obtained by diluting the 0.20 mg/g SMB-11 solution in the presence of 10 mM Na_2SO_4 using pH 4.50 water as for the preparation of other

AFM samples. At both temperatures, the brush molecules were in a three-arm star shape, as expected. The average arm length of SMB-11 molecules from the image analysis was 83.0 ± 31.1 nm at 20 °C (from 120 arms of three-arm star brushes) and 87.5 ± 30.0 nm at 70 °C from 75 arms. These two values were similar to each other but noticeably smaller than those of SMB-11 in the star state under other conditions (e.g., 95.7 ± 33.4 nm in the presence of $NaPF_6$ at 70 °C). The average arm height of SMB-11 was 1.6 ± 0.3 nm at 20 °C (from 200 arms) and 1.8 ± 0.5 nm at 70 °C (from 87 arms), which were slightly larger than that of SMB-11 (1.5 ± 0.3 nm) in the presence of PF_6^- at 70 °C. These observations are likely caused by the bridging interactions of divalent SO_4^{2-} anions with protonated PDMAEMA, resulting in brush shrinking.

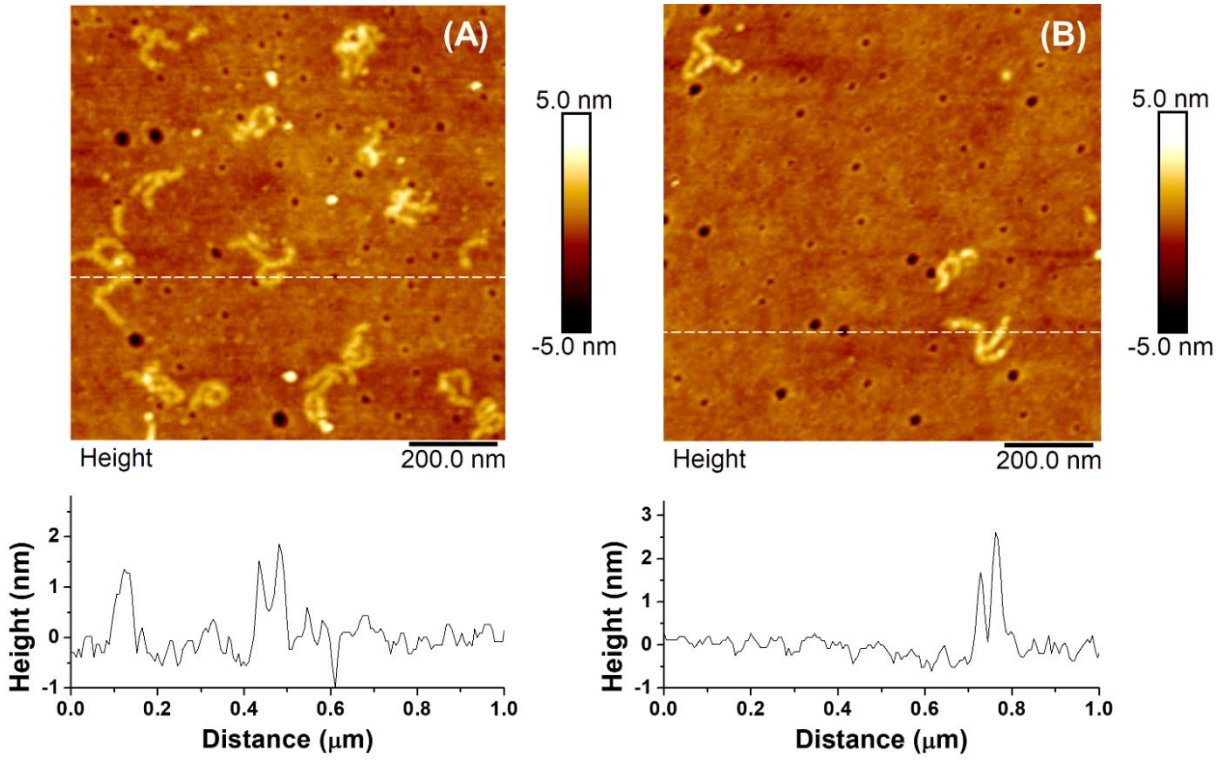

Figure 11. AFM height images of SMB-11 drop cast on glass disks from a solution of 0.050 mg/g SMB-11 in pH 4.50 water with 2.5 mM Na_2SO_4 at 20 °C (A) and 70 °C (B), with a cross-sectional profile along the dashed line in each image. The solution was diluted from a 0.2 mg/g solution of SMB-11 in pH 4.50 water with 10 mM Na_2SO_4 using pH 4.50 water.

Conclusions

In summary, we synthesized two three-arm star-shaped bottlebrush polymers heterografted with 5 kDa PEO and either PDMAEMA (for SMB-11) or PDEAEMA (for SMB-22) and investigated the effects of temperature on super and moderate CA-induced star-globule shape transitions of the two brush polymers in acidic water and the interactions of protonated bottlebrushes with weak CA I^- and kosmotropic anion SO_4^{2-}. Consistent with the previous report, the addition of super CAs, such as $[Fe(CN)_6]^{3-}$ and $[Fe(CN)_6]^{4-}$, and moderate CAs, such as PF_6^- and ClO_4^-, induced starlike-to-globular shape transitions of both SMB-11 and -22 at pH 4.50 at 25 °C due to the chaotropic ion pairing of protonated tertiary amine groups with CAs as well as the chaotropic effect. DLS and AFM studies showed that the globular brushes collapsed by super CAs remained in the globular state when the temperature was increased to 70 °C. In contrast, the star bottlebrushes collapsed by moderate CAs underwent globule-to-star shape changes upon heating. At the same concentration of the same salt, the transition temperature was higher for SMB-22 than SMB-11 likely due to the chaotropic effect. On the other hand, weak CA I^- and kosmotropic anion SO_4^{2-} exerted rather small influences on the conformations of SMB-11 and -22 at 25 °C, and only small size variations were observed upon heating to 70 °C. AFM showed that SMB-11 in the presence of Na_2SO_4 remained in the star shape at both 20 and 70 °C. These findings enrich the fields of stimuli-responsive shape-changing MBBs and chaotropic ion pairing/chaotropic effect-induced supramolecular assembly and might be useful in the design of smart polymer systems for potential applications such as encapsulation and release of substances.

ORCID

Bin Zhao: 0000-0001-5505-9390

Conflicts of interest: There are no conflicts to declare.

Electronic Supplementary Information Available. Experimental section, calculation of grafting densities and $M_{w,cal}$ of SMB-1 and -2, and additional experimental data. The Electronic Supplementary Information is available free of charge on the website at DOI: xxxxxxxxxxxxx.

Acknowledgements: This work was supported by NSF (DMR-1607076 and -2004564).

References:

1. M. Zhang, A. H. E. Müller, *J. Polym. Sci. Part A: Polym. Chem.*, 2005**, 43**, 3461-3481.
2. S. S. Sheiko, B. S. Sumerlin, K. Matyjaszewski, *Prog. Polym. Sci.*, 2008**, 33**, 759-785.
3. H.-i. Lee, J. Pietrasik, S. S. Sheiko, K. Matyjaszewski, *Prog. Polym. Sci.*, 2010**, 35**, 24-44.
4. G. Xie, M. R. Martinez, M. Olszewski, S. S. Sheiko, K. Matyjaszewski, *Biomacromolecules*, 2019**, 20**, 27-54.
5. B. Zhao, *J. Phys. Chem. B*, 2021, **125**, ASAP Article. DOI: 10.1021/acs.jpcb.1c01819.
6. S. S. Sheiko, J. Zhou, J. Arnold, D. Neugebauer, K. Matyjaszewski, C. Tsitsilianis, V. V. Tsukruk, J.-M. Y. Carrillo, A. V. Dobrynin, M. Rubinstein, *Nat. Mater.*, *2013*, **12**, 735-740.
7. W. F. Daniel, J. Burdynska, M. Vatankhah-Varnoosfaderani, K. Matyjaszewski, J. Paturej, M. Rubinstein, A. V. Dobrynin, S. S. Sheiko, *Nat. Mater.*, 2016, **15**, 183−189.
8. J. A. Johnson, Y. Y. Lu, A. O. Burts, Y. Xia, A. C. Durrell, D. A. Tirrell, R. H. Grubbs, *Macromolecules*, 2010, **43**, 10326−10335.
9. X. Banquy, J. Burdyńska, D. W. Lee, K. Matyjaszewski, J. Israelachvili, *J. Am. Chem. Soc.*, 2014**, 136**, 6199-6202.
10. A. L. Liberman-Martin, C. K. Chu, R. H. Grubbs, *Macromol. Rapid Commun.*, 2017, **38**, 1700058.
11. H. Qi, X. T. Liu, D. M. Henn, S. Mei, M. C. Staub, B. Zhao, C. Y. Li, *Nat. Commun.*, 2020, **11**, 2152.
12. S. S. Sheiko, S. A. Prokhorova, K. L. Beers, K. Matyjaszewski, I. I. Potemkin, A. R. Khokhlov, M. Möller, *Macromolecules*, 2001, **34**, 8354−8360.
13. J. R. Boyce, D. Shirvanyants, S. S. Sheiko, D. A. Ivanov, S. H. Qin, H. G. Börner, K. Matyjaszewski, *Langmuir*, 2004, **20**, 6005–6011.
14. M. O. Gallyamov, B. Tartsch, A. R. Khokhlov, S. S. Sheiko, H. G. Börner, K. Matyjaszewski, M. Möller, *Chem. Eur. J.*, 2004, **10**, 4599–4605.
15. C. Li, N. Gunari, K. Fischer, A. Janshoff, M. Schmidt, *Angew. Chem., Int. Ed.*, 2004, **43**, 1101−1104.
16. H.-i. Lee, J. Pietrasik, K. Matyjaszewski, *Macromolecules*, 2006, **39**, 3914−3920.
17. S.-i. Yamamoto, J. Pietrasik, K. Matyjaszewski, *Macromolecules*, 2007, **40**, 9348−9353.
18. J. Pietrasik, B. S. Sumerlin, R. Y. Lee, K. Matyjaszewski, *Macromol. Chem. Phys.*, 2007, **208**, 30−36.
19. H.-i. Lee, J. R. Boyce, A. Nese, S. S. Sheiko, K. Matyjaszewski, *Polymer*, 2008, **49**, 5490−5496.

20. X. Li, H. ShamsiJazeyi, S. L. Pesek, A. Agrawal, B. Hammouda, R. Verduzco, *Soft Matter*, 2014, **10**, 2008−2015.
21. E. Kutnyanszky, M. A. Hempenius, G. J. Vancso, *Polym. Chem.*, 2014, **5**, 771−783.
22. X. M. Zhu, J. Zhang, C. Miao, S. Y. Li, Y. L. Zhao, *Polym. Chem.* 2020, **11**, 3003-3017.
23. Y. Y. Xu, S. Bolisetty, M. Drechsler, B. Fang, J. Yuan, M. Ballauff, A. X. E. Müller, *Polymer*, 2008, **49**, 3957−3964.
24. Y. Y. Xu, S. Bolisetty, M. Ballauff, A. X. E. Müller, *J. Am. Chem. Soc.*, 2009, **131**, 1640−1641.
25. N. Gunari, Y. Cong, B. Zhang, K. Fischer, A. Janshoff, M. Schmidt, *Macromol. Rapid Commun.*, 2008, **29**, 821−825.
26. Y. Cong, N. Gunari, B. Zhang, A. Janshoff, M. Schmidt, *Langmuir*, 2009, **25**, 6392–6397.
27. Y. Y. Xu, S. Bolisetty, M. Drechsler, B. Fang, J. Yuan, L. Harnau, M. Ballauff, A. H. E. Müller, *Soft Matter*, 2009, **5**, 379−384.
28. Y. Y. Xu, O. V. Borisov, M. Ballauff, A. X. E. Müller, *Langmuir* 2010, **26**, 6919–6926.
29. D. M. Henn, W. X. Fu, S. Mei, C. Y. Li, B. Zhao, *Macromolecules*, 2017, **50**, 1645-1656.
30. D. M. Henn, C. M. Lau, C. Y. Li, B. Zhao, *Polym. Chem.*, 2017, **8**, 2702-2712.
31. D. M. Henn, J. A. Holmes, E. W. Kent, B. Zhao, *J. Phys. Chem. B*, 2018, **122**, 7015-7025.
32. E. W. Kent, B. Zhao, *Macromolecules*, 2019, **52**, 6714-6724.
33. H. Luo, M. Szymusiak, E. A. Garcia, L. L. Lock, H. Cui, Y. Liu, M. Herrera-Alonso, *Macromolecules*, 2017, **50**, 2201−2206.
34. E. A. Garcia, H. Y. Luo, C. E. Mack, M. Herrera-Alonso, *Soft Matter*, 2020, **16**, 8871-8876.
35. B. Gumus, M. Herrera-Alonso, A. Ramírez-Hernández, *Soft Matter*, 2020, **16**, 4969-4979.
36. E. W. Kent, E. M. Lewoczko, B. Zhao, *Polym. Chem.*, 2021, **12**, 265-276.
37. E. W. Kent, D. M. Henn, B. Zhao, *Polym. Chem.*, 2018, **9**, 5133-5144.
38. R. A. Gumerov, I. I. Potemkin, *Colloid Polym. Sci.*, 2021, **299**, 407-418.
39. K. D. Collins, *Biophys. J.*, 1997, **72**, 65-76.
40. Y. Marcus, *Chem. Rev.*, 2009, **109**, 1346–1370.
41. Y. Marcus, G. Hefter, *Chem. Rev.*, 2006, **106**, 4585-4621.
42. L. D. Liu, R. Kou, G. M. Liu, *Soft Matter*, 2017, **13**, 68-80.
43. K. I. Assaf, W. M. Nau, *Angew. Chem. Int. Ed.* 2018, **57**, 13968–13981.
44. F. A. Plamper, A. Schmalz, M. Ballauff, A. H. E. Müller, *J. Am. Chem. Soc.*, 2007, **129**, 14538-14539.
45. Q. Zhang, F. Tosi, S. Ügdüler, S. Maji, R. Hoogenboom, *Macromol. Rapid Commun.*, 2015, **36**, 633−639.
46. P. Flemming, M. Müller, A. Fery, A. S. Münch, P. Uhlmann, *Macromolecules*, 2020, **53**, 1957-1966.
47. E. Karjalainen, V. Aseyev, H. Tenhu, *Macromolecules*, 2014, **47**, 7581−7587.
48. X. Cao, Z. An, *Macromol. Rapid Commun.*, 2015, **36**, 2107−2110.
49. H. Tang, Y. Li, S. H. Lahasky, S. S. Sheiko, D. H. Zhang, *Macromolecules*, 2011, **44**, 1491−1499.
50. P. Zhao, Y. Yan, X. Feng, L. Liu, C. Wang, Y. Chen, *Polymer*, 2012, **53**, 1992-2000.
51. E. W. Kent, E. M. Lewoczko, B. Zhao, *Langmuir,* 2020, **36**, 13320-13330.
52. K. J. Zhou, Y. G. Wang, X. N. Huang, K. Luby-Phelps, B. D. Sumer, J. M. Gao, *Angew. Chem. Int. Ed.*, 2011, **50**, 6109−6114.
53. D. M. Henn, R. A. E. Wright, J. W. Woodcock, B. Hu, B. Zhao, *Langmuir*, 2014, **30**, 2541–2550.

54. Y. Li, Y. G. Wang, G. Huang, X. P. Ma, K. J. Zhou, J. M. Gao, *Angew. Chem. Int. Ed.*, 2014, **53**, 8074 –8078.
55. L.-H. Wang, Z.-D. Zhang, C.-Y. Hong, X.-H. He, W. You, Y.-Z. You, *Adv. Mater.*, 2015, **27**, 3202–3207.
56. Odian, G. *Principles of Polymerization*, 4th ed.; John Wiley & Sons, Inc.: New Jersey, 2004.
57. D. J. Li, J. R. Dunlap, B. Zhao, *Langmuir*, 2008, **24**, 5911-5918.
58. P.-Y. Hsiao, E. Luijten, *Phys. Rev. Lett.*, 2006, **97**, 148301.
59. A. Kundagrami, M. Muthukumar, *J. Chem. Phys.*, 2008, **128**, 244901.
60. P. X. Jia, J. Zhao, *J. Chem. Phys.*, 2009, **131**, 231103.

For Table of Contents Graphic Use Only

Title: Effects of Temperature on Chaotropic Anion-Induced Shape Transitions of Star Molecular Bottlebrushes with Heterografted Poly(ethylene oxide) and Poly(*N*,*N*-dialkylaminoethyl methacrylate) Side Chains in Acidic Water

Authors: *Evan M. Lewoczko, Michael T. Kelly, Ethan W. Kent, and Bin Zhao*

Table of Content Entry Graphic

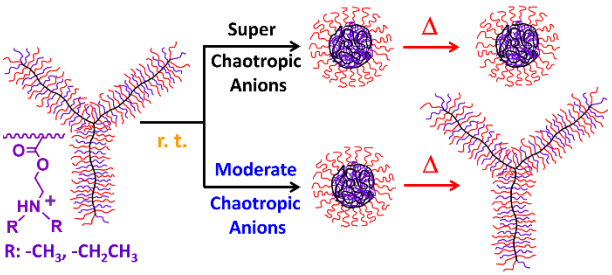

Table of Contents Entry Graphical Abstract: While super chaotropic anion (CA)-collapsed protonated tertiary amine-containing three-arm star bottlebrushes remain globular upon heating from room temperature to 70 °C, moderate CA-collapsed bottlebrushes exhibit star-globule shape transitions.